Sensors and Materials, Vol. 38, No. 8 (2026) 4833–4844 4833
MYU Tokyo

S & M 4596

Monitoring of Land Use Change within the Red Line of Ecological Protection in Beijing

Yi Zhang,[1,2,4*] Siyang Yin,[1,2,4] Yu Liu,[3] Shuang Wu,[1,2,4] and Yuan Zhuang[1,2,4]

[1]Beijing Institute of Surveying and Mapping, Beijing 100045, China
[2]Beijing Key Laboratory of Urban Spatial Information Engineering, Beijing 100038, China
[3]Beijing Fengtai District Real Estate Registration Service Center, Beijing 100071, China
[4]Beijing Society of Surveying and Mapping, Beijing 100038, China

(Received July 31, 2024; accepted June 18, 2026)

Keywords: ecological protection red line, land cover, change monitoring, spatial identification, Moran's I

In this study, we analyze the spatial changes in land surface cover within Beijing's ecological protection red line using geographic national survey and monitoring data from 2015, 2017, and 2019. Through global and local Moran's I spatial autocorrelation methods, we identify regions of intensive human activity, significant ecological restoration, and notable ecological degradation within the protected zones. According to the principle of "what you see is what you get", the surface coverage within the ecological protection red line is divided into two categories and eight subcategories, and the land-use transfer matrix and land-use dynamics model are used to qualitatively determine the changes in land cover type within the ecological protection red line. Quantitative change extraction and analysis are conducted by taking each vector patch that has changed as the research unit, taking ecological and non-ecological land outflow patches as research subjects, calculating Moran's I index to measure the spatial correlation, and detecting them separately. The spatial correlation among changed patches can thus be used to identify areas of intensive human activity within the ecological protection red line. Studies have shown that the ecological land within the ecological protection red line from 2015 to 2019 is in an outflow state as a whole, and various changed patches have obvious spatial autocorrelation effects. Fifteen areas show high human activities, including Wuling Mountain and the surrounding mountains. Significant signs of man-made damage have occurred in six areas in Songshan, namely, the Yudu Mountain Reserve, the Nanhaizi Park, the Miyun Reservoir, the Huaisha Huaijiu River, and the Pinggu section (southwest section) of the Yanghe River. It is recommended to increase the supervision of the above areas and implement significant ecological restoration. The Miyun section of the Jingmi Water Diversion Canal and eight other areas all coexist with man-made destruction and repair activities. The research provides a decision-making basis for strictly observing the red line of ecological protection, accelerating the construction of beautiful sites in Beijing and the construction of ecological civilization. The research method is also applicable to the monitoring of changes in land surface cover within the red line of ecological protection in other regions of the country.

*Corresponding author: e-mail: 1113611326@qq.com
https://doi.org/10.18494/SAM5457

ISSN 0914-4935 © MYU K.K.
https://myukk.org/

1. Introduction

The ecological protection red line is an important institutional innovation in China's environmental protection.(1) Following the "120 million hectares farmland red line," it represents another national "lifeline".(2–4) Delineating the red line is the foundation, strictly adhering to the red line is the key,(5) and building a national land ecological security barrier is an important task for the construction of ecological civilization, the construction of the capital's ecological environment, and the high-quality development of the capital.(6)

At present, there are only a few studies on the monitoring of surface coverage changes and human activities within the red line, which is not conducive to the supervision of the ecological protection red line and the implementation of relevant national ecological protection policies. Brown and Duh(7) proposed a method to simulate the land cover pattern on the basis of historical land use maps and planning documents, which can reflect the ecological and environmental impacts in the study area. On the basis of the long time series of land use and land cover data, Hu and Batunacun(8) and Wang *et al.*(9) used the transfer matrix and Markov chain to obtain the model, process, and spatial autocorrelations of land use and land cover in the study area. On the basis of the delineation results of the ecological protection red line, Xie(10) discussed the methods and principles of land use zoning based on the ecological protection red line and combined with the relevant theories and methods of land use zoning. Zhu *et al.*(11) and Chen *et al.*(12) used the Conversion of Land Use and its Effects at Small regional extent (CLUE-S) model to simulate the future land use changes in the Liangjiang New Area of Chongqing under the protection of the ecological red line, and they constructed the optimization model for ecosystem service value evaluation to analyze the sensitivity and change degree of ecosystem service value. Rao *et al.*(13) studied the land use change in the Wanzhou District of Chongqing City in 2025 using the Future Land Use Simulation (FLUS) model under the ecological red line constraint. The total value of ecosystem services was calculated using the ecological value coefficient and land use change, and the effects of different land value coefficients and areas on the total value were analyzed.

This study innovatively applies spatial autocorrelation analysis to monitor human activities within the ecological conservation red line. By separately examining the spatial autocorrelation of changing patches in both ecological and non-ecological land, we reveal the potential dependencies and interactions among them. This approach effectively maps the spatial distribution patterns of these changes. On the basis of the results of the analysis, we identify areas with a significant aggregation effect where non-ecological land is converted to ecological uses and, conversely, where ecological land is lost to non-ecological uses. The findings facilitate more targeted and efficient land-use regulation and supervision within the red line, offering valuable insights for other regions pursuing Sustainable Development Goals while conserving natural resources.

2. Materials and Methods

2.1 Study area

Beijing is located in the transition zone of the mountainous plain and the intersection of the Taihang Mountain and the Yanshan Mountain system. The center is located in the east at longitude 116°20 ‘and north latitude 39°56’, with a total area of about 16410 square kilometers. The terrain is high in the northwest and low in the southeast, belonging to the Haihe River basin with more than 400 rivers, forming five water systems: the Yongding River, Chaobai River, Daqing River, North Canal, and Ji Canal. The transitional topography and landforms of mountains and plains make the ecosystem diverse and rich in biodiversity.

The red line of ecological protection in Beijing covers a total area of about 4,290 square kilometers, accounting for 26.1% of the regional area of Beijing, showing the spatial distribution patterns of “two screens and two belts”. The pattern “two screens” refers to the Yanshan ecological barrier in the north and the ecological barrier of the Taihang Mountain in the west, and the pattern “two belts” refers to the Ecological Conservation Belt along the Yongding River and the Ecological Conservation Belt along the Chaobai River and the Grand Canal. The map of the study area is shown in Fig. 1.

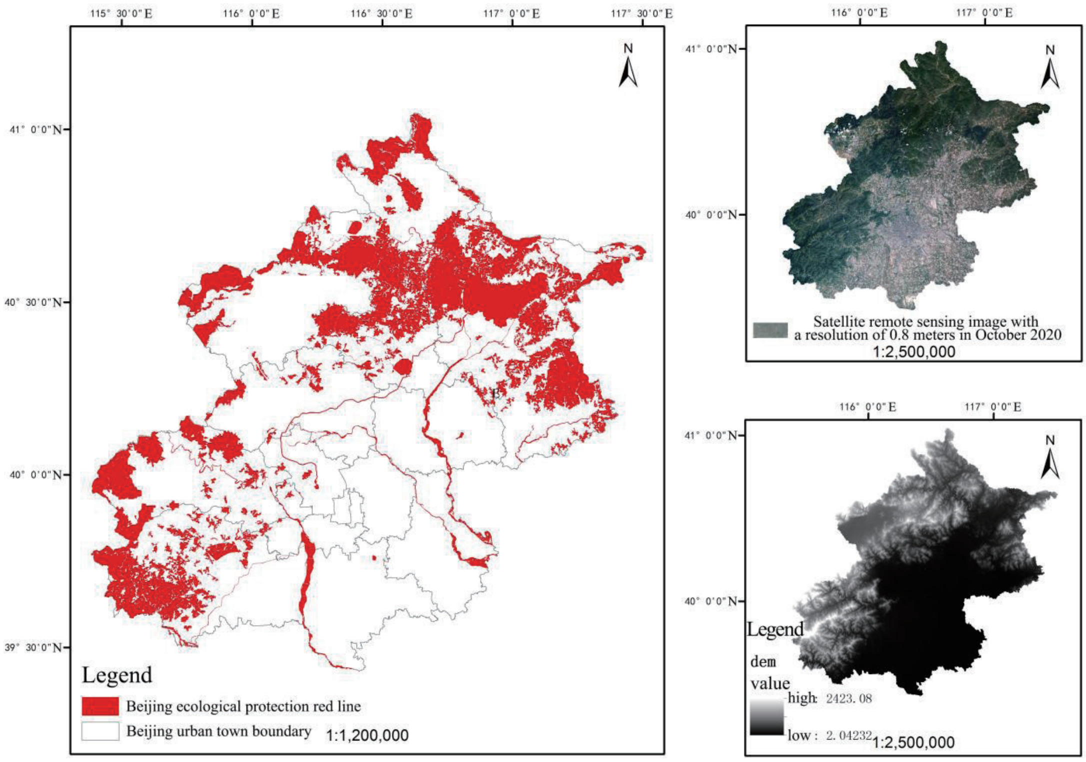

Fig. 1. (Color online) Map of study area.

2.2 Data sources

The data of the ecological protection red line are from the Beijing Ecological Environment Bureau; the geographical national survey and monitoring data in 2015, 2017, and 2019, and the data of plains and shallow and deep mountains are from the Beijing Planning and Natural Resources Commission.

2.3 Land-use transfer matrix

The land use transfer matrix can describe the area changes of land use types and the change of transfer between different types of land in two periods.(14) It enables a comprehensive and concrete analysis of the changes in quantitative structure characteristics and the changes in the directions of various types of land use.

$$P_{ij} = \frac{S_{ij}}{\sum_{i=1}^{n}\sum_{j=1}^{n} S_{ij}} \tag{1}$$

Here, P_{ij} is the probability of land use type i being converted to j between 2015 and 2019, and S_{ij} represents the area of land converted from type i to type j.

On the basis of the ecological function, land within the ecological conservation red line is classified into two broad categories: ecological land and non-ecological land. Following the principle of "what you see is what you get" (i.e., classification by directly observable land cover characteristics), ecological land is further divided into three types: cultivated land, woodland and grassland, and water bodies. Non-ecological land is subdivided into five types: built-up areas, railways and roads, structures, artificially excavated or deposited land, and bare land.

2.4 Moran's I spatial autocorrelation test

In space, a space unit and other space units around it have a certain attribute called space autocorrelation, that is, the closer the spatial position points, the more similar corresponding variables may be. Testing whether the attribute value is significantly associated with an important index reveals the similarity between adjacent space unit properties, that is, their correlation. As a geographical entity, the surface cover change patch within the red line may have certain distribution rules in space.(14) To this end, it is necessary to test whether spatial autocorrelation exists from spatial management. Moran's I is the most commonly used effective indicator to detect the magnitude of variable spatial autocorrelation, with a value domain range of [−1,1], with negative values representing a regional spatial negative correlation, positive values representing a regional spatial autocorrelation, and zero values representing random spatial distributed states.(15–17) The spatial autocorrelation is divided into global and localized spatial autocorrelations.(18,19)

According to the objectives of this study, the area of an ecological land that became a non-ecological land is defined as the area with ecological destruction, and the area with significant changes is defined as the area with significant ecological destruction by Moran's I test; the area of a non-ecological land that became an ecological land is defined as the ecological restoration area, and the area with significant changes is defined as the area with significant ecological restoration by Moran's I test.

2.4.1 Global spatial autocorrelation

Global spatial autocorrelation describes the overall distribution of a phenomenon. It can be judged whether the phenomenon exists in a specific region, but not the spatial distribution of a cluster area.

The global space autocorrelation can be expressed as

$$I = \frac{N}{\sum_i \sum_j w_{ij}} \frac{\sum_i \sum_j w_{ij}(x_i - \bar{x})(x_j - \bar{x})}{\sum_i (x_i - \bar{x})^2}. \tag{2}$$

Here, N denotes the number of spatial units; x_i and x_j represent the attribute values at spatial locations i and j, respectively; $\bar{x}$ is the mean of the attribute across all spatial locations; w_{ij} represents the spatial weight matrix.

2.4.2 Local spatial autocorrelation

The local spatiotemporal Moran's I index describes the spatiotemporal aggregation pattern of changing patches. It is used to calculate the local spatial aggregation and can indicate the spatial distribution of clusters.[20,21]

The local spatial autocorrelation can be expressed as

$$I_i = \left[\frac{x_i - \bar{x}}{\sum_{j \neq i}^{N} \frac{X_j^i}{(N-1)} - \bar{x}^2} \right] \sum_{j=1}^{N} W_{ij} \left(X_i - \bar{x} \right). \tag{3}$$

Here, I_i is the local spatial autocorrelation coefficient and the other symbols have the same meaning as in Eq. (2).

Moran's I index is standardized by the Z-score method to test the positive correlation and significance, which can be expressed as

$$Z_{ij} = \frac{I_{ij} - \mu_{ij}}{\delta_{ij}}. \tag{4}$$

Here, I_{ij}, μ_{ij}, and δ_{ij} are the Moran's I index, expected value, and variance, respectively. When the value is greater than 1.96 or less than −1.96, the sample spatial correlation is significant at 0.05.

That is, there is spatial autocorrelation of the study variable in the region when the value range is [−1.96,1.96]; otherwise, the correlation of the study variable is not significant, that is, the autocorrelation is weak.

3. Results

3.1 Land-use transfer matrix

The land-use transfer matrix is a quantitative description of the transfer change of various land-use types within the ecological protection red line from 2015 to 2019. In this study using A rcGIS10.1, the matrix operations, and the statistical analysis, the surface cover was classified on the basis of two major categories and eight subcategories, according to the land-use transfer matrix formula, using the land-use transfer matrix within the red line from 2015 to 2019. As shown in Table 1, the conversion of ecological land to non-ecological land is greater than that of non-ecological land to ecological land in 2015–2019. Regarding the state of ecological land with a small amount of outflow, the coverage area of forest and grass is obvious. The transformation of planting vegetation, piling surfaces, structures, and bare land to forest and grass cover is obvious. Since 2000, it has been Beijing's policy to transform farmland back into forest to improve the ecological environment, reduce soil and water loss, optimize the rural industrial structure,[22] and increase the farmers' income, which were important goals. In 2012, the afforestation project was started involving millions of mu of land to further expand the green

Table 1
Area of land-use transfer matrix within the red line from 2015 to 2019.

		2019								
		Ecological land (km^2)			Non-ecological land (km^2)					
		Forest grass cover	Planting vegetation	Waters	Digging surfaces	Housing construction area	Structures	Bare surfaces	Railways and roads	Total
2015										
Ecological land	Forest grass cover	3604.40	10.90	33.10	6.04	0.70	3.86	1.64	2.20	3662.85
	Planting vegetation	36.89	301.56	12.62	1.72	0.59	1.41	0.20	0.91	355.89
	Waters	1.91	0.09	170.40	0.59	0.01	0.27	0.04	0.04	173.35
	Subtotal		4171.86				20.22			
Non-ecological land	Digging surfaces	5.67	0.49	1.35	6.19	0.08	0.42	0.09	0.23	14.53
	Housing construction area	0.72	0.23	0.01	0.69	10.60	0.32	0.00	0.05	12.62
	Structures	3.41	1.06	0.67	0.75	0.23	10.62	0.12	0.25	17.11
	Bare surfaces	3.25	0.07	1.18	2.21	0.01	0.13	26.29	0.21	33.35
	Railways and roads	0.51	0.07	0.26	0.14	0.03	0.11	0.02	18.32	19.45
	Subtotal		18.96				78.11			
	Total	3656.76	314.47	219.59	18.35	12.24	17.14	28.40	22.20	4289.15

ecological space, optimize the structure of green space, and improve the quality of the ecological environment; the forest cover area may be affected by transforming farmland back to forest with this afforestation project. In the transformation of ecological land to non-ecological land, the land flow into the surface of a pile is obvious, and the flow into the building area is the least, which to some extent reflects the strict control of human activities within the red line.

3.2 Global Moran's I spatial autocorrelation test

By the extraction of the change map spots from 2015 to 2019 using ArcGIS, the patches of ecological land and non-ecological land from 2015 to 2019 were identified as study subjects, and the global spatial autocorrelation test was conducted. From Table 2, Moran's I index of both types of change patches was greater than 0, the Z-score was greater than 1.96, and the P-value was greater than 0 but close to 0. Test results show that in 2015–2019, the ecological protection line within the scope of all changed patches shows significant space autocorrelation, the aggregation phenomenon, the same space scope, the improvement of ecological space, and the destruction of the aggregation joint effect. Among these findings, the ecological land conversion is the most obvious, which reflects the ecological restoration project characteristics of large and small areas.

3.3 Local Moran's I spatial autocorrelation test

The local spatiotemporal Moran's I was computed for local spatiotemporal aggregation maps. Taking ecological land-non-ecological land and non-ecological land-ecological land as research subjects, we conducted the local spatial autocorrelation analysis to identify the spatial location and the degree of aggregation of various changed patches. Two types of subjects were tested for significance, and drop plots of local spatial autocorrelation were made. In the significance map, "non-significant" indicates an insignificant spatial autocorrelation, and the larger the P-value, the higher the spatial autocorrelation. In the aggregation map, high–high and low–low aggregation patterns represent a significant spatial autocorrelation, high–low and low–high aggregation patterns represent a spatial anomaly, and "non-significant" indicates a discrete spatial distribution pattern.

(1) Inspection of the local space autocorrelation of patches with the ecological land-to-non-ecological land change: Taking the transformation of ecological land to non-ecological land

Table 2
Global Moran's I index values of all surface cover changes from 2015 to 2019 in Beijing.

Index number	Change rate	
	Ecological land-to-non-ecological land-use change	Non-ecological land-to-ecological land-use change
Moran's I	0.033	0.021
Z-score	27.906	13.062
P-value	0.001	0.001

as the research object, the human construction activities within the ecological protection red line were analyzed from 2015 to 2019. Figure 2 shows the results of the significance analysis of patches with an ecological land-to-non-ecological land change. It can be seen from Fig. 2 that of the 15,178 patches studied, 7407 showed the change that passed the significance test. The areas showing the most significant spatial correlation are concentrated in Guanting Reservoir, Nanhaizi Park, the Daxing section of the Yongding River, the middle and southern sections of the Juma River in Fangshan District, the Juhe Pinggu section (southwest section), Yoda Lake Nature Reserve, and Sizuolou Nature Reserve. Human activities in the above protected areas are relatively concentrated and the aggregation effect is obvious. Figure 3 shows the results of the analysis of patches with the ecological land-to-non-ecological land change. It can be seen from the figure that the southern section of the Juma River in Fangshan District, the Yongding River Daxing section, Nanhaizi Park, the Juhe Pinggu section (southwest section), Duck Lake Nature Reserve, and other places have a significant high–high aggregation form. This reflects the existence of a large area of human non-ecological construction activities in the above areas. Guanting Reservoir, Sizuolou Nature Reserve, the middle section of the Juma River in Fangshan District, Yongding River Fangshan, the Changping section, and the southwest of Miyun have a significant low–low aggregation

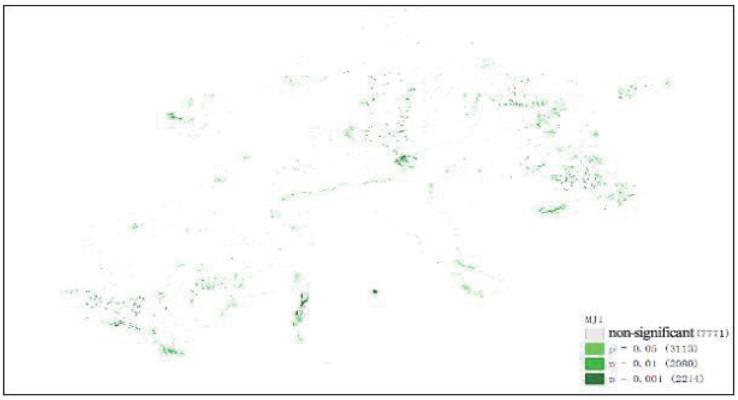

Fig. 2. (Color online) Significance map of patches with ecological land-to-non-ecological land change.

Fig. 3. (Color online) Aggregation map of patches with ecological land-to-non-ecological land change.

form. This finding is indicative of small-scale, clustered, anthropogenic non-ecological construction activities in the aforementioned regions.

(2) Local spatial autocorrelation test of patches with non-ecological land-to-ecological land change: The patches transformed from non-ecological land to ecological land, including afforestation and the transformation of farmland back into forest in the ecological protection red line from 2015 to 2019, were analyzed. It can be seen from Fig. 4 that of the 8,184 patches subjects studied, 3905 patches show the change that passed the significance test, The areas with the most significant spatial correlation are concentrated in the Daxing section of the Yongding River, the Fangshan section of the Juma River, the Fangshan section of the main canal of the South-to-North Water Diversion Project, the Fangshan section of Beijing-mi Diversion Canal, the Changping section, the Miyun section, Guanting Reservoir, Shihua Cave Nature Reserve, the northwest Miyun Mountain area, and Sizuolou Nature Reserve. The above areas are where ecological restoration is concentrated. The aggregation effect is obvious. Figure 5 shows the results of the analysis of patches with a non-ecological land-to-ecological land change. It can be seen from Fig. 5 that the Daxing section of the Yongding River, the Fangshan section of the Juma River (south section), the Miyun section of Jingmi Diversion Canal, the Changping section, and other places have a significant high–high aggregation form. This reflects obvious effects in the above areas in recent years undergoing the conversion of farmland back to forest, afforestation, and other ecological restoration activities. The Fangshan West Mountain area, Shihua Cave Nature Reserve, the Fangshan section of the main canal of the South-to-North Water Diversion Project, the Shunyi section of Jingmi Diversion Canal, Guanting Reservoir, the Miyun northwest mountain area, and Sizuolou Nature Reserve have a significant low-low aggregation form. This reflects that the above areas have carried out small- and large-range ecological restoration work. The ecological restoration effect is remarkable.

3.4 Identification of areas with intensive human construction activities and significant ecological restoration areas

This study identified a total of 15 areas characterized by either intensive human activity or significant ecological restoration. Among these, six sites were designated as significant

Fig. 4. (Color online) Significance map of patches with non-ecological land-to-ecological land change.

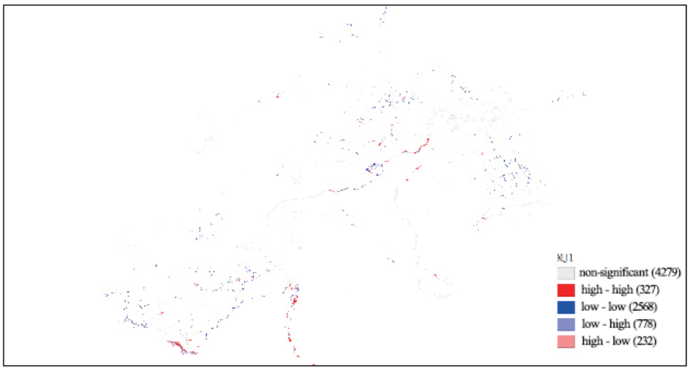

Fig. 5. (Color online) Aggregation map of patches with non-ecological land-to-ecological land change.

Table 3
Identification of areas showing significant changes within the ecological conservation red line.

Order number	Significant amount of change in clustered areas	Ecological land-to-non-ecological land-use change		Non-ecological land-to-ecological land-use change	
		High–high	Low–low	High–high	Low–low
1)	Sizuolou Nature Reserve		√		√
2)	Shihua Cave Nature Reserve		√		√
3)	Wuling Mountain and surrounding mountains		√		
4)	Songshan and Yudu Mountain protected areas	√			
5)	Nanhaizi Park	√			
6)	Northwest Miyun Mountain area		√		√
7)	Fangshan District, southwest mountain area		√		√
8)	Miyun Reservoir		√		
9)	Guanting Reservoir		√		√
10)	Huaisha River, Huaijiu River		√		
11)	Fangshan Section (south section)	√		√	
12)	Daxing section of Yongding River	√		√	
13)	Juhe Pinggu section (southwest section)	√			
14)	Miyun section of Jingmi Diversion Canal			√	
15)	Shunyi section of Jingmi Diversion Canal		√		√

ecological degradation areas: the Songshan and Yudu Mountain Nature Reserves, Nanhaizi Park, the southwestern section of the Ju River in Pinggu District, the Wuling Mountain area and its surrounding region, Miyun Reservoir, and the Huaisha-Huaijiu River area. One area, the Miyun section of Jing-Miyun Diversion Canal, was recognized as a significant ecological restoration site. The remaining identified areas are regions where significant degradation and restoration coexist. The specific areas identified and their situation are shown in Table 3.

4. Conclusions

In this study, using the ArcGIS spatial analysis technique, the spatial autocorrelation model, and the results of the geographical national surveys and monitoring in 2015, 2017, and 2019, the surface cover types within the ecological protection red line are classified into two categories and eight subcategories. The changing vector unit is used as the study unit, with the outflow of ecological land into patches. The spatial identification of ecological restoration and non-ecological human activities within the ecological protection red line was conducted. An analysis was performed to examine the dependencies and mutual influences among the patches of land cover change within the ecological conservation red line. The analysis results show that from 2015 to 2019, there were clear spatial autocorrelation effects in various patches within the red line. In this study, we identified a total of 15 human activity-intensive areas within the red line, six areas with significant ecological damage, and one area with significant ecological restoration. All other areas showed the coexistence of destruction and repair.

This study complements the research gap in the characteristic analysis of human activities in a short-time series within the red line, which makes the land use control and supervision within the red line more targeted and efficient. The findings of this study will also promote the construction of ecological civilization and the implementation of ecological protection and supervision tasks in Beijing.

References

1 A. Q. Song Ed.: A Study on the Legal System of Ecological Redline (Jilin University, China, 2019).
2 Finance & Accounting for Communications (2016) 67. https://kns.cnki.net/kcms2/article/abstract?v=A2Z-m-A1gcnF-ZYKfXXc7jtSk0V-AgImZnsRgO7Jfdey31waPteI0epLqZQzzd8spLzoP5Tneu7TPlxTEv-6x5qSrM3-HxuyvFYDzUVReQQbe6sTFW1d7oWD61Qnun-Pwy5HLiPUzuMN-FCx6XP4CpPokDGPMcPNjoNYbow6sMIVt-hafgX1YgScY36zCeUOHLAwMv0yvur-Xy_iusEWaA==&uniplatform=NZKPT&language=CHS
3 S. Rao, Q. Zhang, and X. J. Mou: J. Environ. Econ. **11** (2012) 57.
4 J. C. Huang, H. X. Lin, and X. X. Qi: Prog. Geogr. **36** (2017)378.
5 L. X. Wang, C. X. Zhou, Y. Wang, N. F. Lin, D. Wu, H. Jiang, and D. L. Xu: Acta Ecol. Sin. **37** (2017) 6176.
6 X. H. Hou Ed.: Research on the Coordinated Demarcation of "Three Lines" under the Background of Ecological Civilization (China University of Geosciences, Wuhan, 2017).
7 D. G. Brown and J. D. Duh: Int. J. Gepgr. Inf. Sci. **18** (2004) 35.
8 Y. F. Hu, Batunacun: Appl. Sci. **8** (2018) 1524. https://doi.org/10.3390/app8091524
9 Y. Wang, S. Zhang, H. Zhen, X. E. Chang, R.Shataer, and Z. Li: Sustainability **12** (2020) 7759. https://doi.org/10.3390/su12187759
10 Y. B. Xie: Zhejiang University (2015). https://kns.cnki.net/kcms2/article/abstract?v=R4S5WDEiKcvAeJ_-vCbrpjZWkbpf7S3A1Mg0cCSPzmeBmA770OpI63Ifhz_4nCUScaE_SuwcP48rQ1ROIABPcwYgnf_emqM1FWLLD_qhCUSMUxwP3CYK-Ej28BZGBg_CgtAw0ydvq-ynu89rPW4oJQCSTtILgQlAQHyjrHwt3wI_A-O0Sb5eOw_QBYes6QKjy32JUxDnkY3HUv8BkKhT7A==&uniplatform=NZKPT&language=CHS
11 K. W. Zhu, B. Lei, Y. C. Li, J. He, and C. H. Yang: Res. Environ. Sci. **30** (2017) 1801. https://doi.org/10.13198/j.issn.1001-6929.2017.03.07
12 B. F. Chen, T. J. Liao, and L. K. Zhang: Res. Soil Water Conserv. **27** (2020) 353. https://doi.org/10.13869/j.cnki.rswc.2020.05.044
13 Y. H. Rao, J. J. Zhang, Q. Xu, and Y. H. Geng: Stat. Decis. **32** (2016) 135. https://doi.org/10.13546/j.cnki.tjyjc.2016.20.035
14 L. Sun, J. Shan, L. J. Mao, X. J. Huang, and Z. M. Wang: J. Jiangsu J. Agric. Sci. **32** (2016) 4060. https://link.cnki.net/urlid/32.1213.S.20161107.1101.034
15 Y. Q. Li, Y. F. Liu, and X. Tang: Sci, Surv. Mapping. **41** (2016) 72. https://doi.org/10.16251/j.cnki.1009-2307.2016.11.014
16 J. H. Wang, Q. M. Qin, C. Du, Z. G. Pang, J. E. Fu, Y. J. Sun, and X. P. Zheng: Sci. Surv. Mapping. **40** (2015) 26. https://doi.org/10.16251/j.cnki.1009-2307.2015.10.005

17 W. H. Li and H. Han: Sci. Surv. Mapping. **43** (2018) 45. https://doi.org/10.16251/j.cnki.1009-2307.2018.02.009
18 M. L. Zheng, H. L. Yang, J. H. Peng, J. H. Wei, and B. B. Zhao: Sci. Surv. Mapping. **44** (2019) 76. https://doi.org/10.16251/j.cnki.1009-2307.2019.05.013
19 Y. P. Ma, S. M. Tan, Z. Y. Lu, and Z. K. Feng: Sci. Surv. Mapping. **43** (2018) 58. https://doi.org/10.16251/j.cnki.1009-2307.2018.03.010
20 S. B. Bi, L. Wan, X. Shen, C. C. Chen, and Y. C. Gong: Sci. Surv. Mapping. **43** (2018) 87. https://doi.org/10.16251/j.cnki.1009-2307.2018.05.015
21 L. J. Wang, Z. Hua, Y. Z. Chen, and B. B. Huang: Glob. Ecol. Conserv. **56** (2024) e03306. https://doi.org/10.1016/j.gecco.2024.e03306
22 Z. Y. Zhang, Y. X. Zhu, and P. H. Jia: Land **13** (2024) 1292. https://doi.org/10.3390/land13081292

About the Authors

Yi Zhang received her B.S. degree from Wuhan University in 2015 and her M.S. degree from China University of Geosciences (Beijing) in 2018. Her research interest covers the application of surveying and mapping geographic big data. (1113611326@qq.com)

Siyang Yin received her B.S. from Shandong University of Science and Technology and her M.S. from the Institute of Remote Sensing and Digital Earth (RADI), CAS. She earned her Ph.D. from Beijing Normal University in 2023 and is currently with the Beijing Institute of Surveying and Mapping. Her research focuses on vegetation remote sensing and land surface classification. (yinsiyang_1@163.com)

Yu Liu received his B.S. and M.S. degrees from China University of Geosciences (Beijing) in 2016 and 2019, respectively. His research interests cover the policy and application of real estate registration. (921368971@qq.com)

Shuang Wu received her B.S. and M.S. degrees from Harbin Normal University, China, in 2011 and 2014, respectively. She received her Ph.D. degree from Beijing Normal University, China, in 2021. Since 2021, she has been working at Beijing Institute of Surveying and Mapping. Her research interests are in urban spatial analysis, climate change, and sensors. (Shuang_1988@hotmail.com)

Yuan Zhuang received her Bachelor of Engineering degree from Northwest A&F University in 2017 and her Master of Engineering degree from Wuhan University in 2020. Since 2020, she has been working at the Beijing Institute of Surveying and Mapping. Her research interests include urban spatial analysis and geographic information science. (419992776@qq.com)